CIVIL ENGINEERING JOURNAL

Article no. 24

THE CIVIL ENGINEERING JOURNAL 3-2023

HISTORICAL RETAINING WALLS MONITORING: A CASE STUDY OF DEBOSQUETTE WALL OF KYIV-PECHERSK LAVRA

Roman Shults[1], Mykola Bilous[2] and Andrii Khailak[3]

1. *King Fahd University of Petroleum and Minerals, Interdisciplinary Research Center for Aviation and Space Exploration, Dhahran, Academic Belt, Bld. 76, Saudi Arabia; roman.shults@kfupm.edu.sa*
2. *Kyiv National University of Construction and Architecture, School of GIS and Territory Management, Department of Applied Geodesy, Povitroflotskij Ave, 31, Kyiv, Ukraine; bilous.mv@knuba.edu.ua*
3. *Research Institute of Building Production named after V.S. Balitsky, Department of Instrumental Control of Construction and Mounting Works, Sector of research, geodetic engineering development and implementation of control methods in construction Lobanovskyi Ave, 51, Kyiv, Ukraine; akhailak79@gmail.com*

ABSTRACT

Geospatial monitoring of historic buildings has a valuable meaning for their restoration and preservation measures. The preparation and accomplishment of such monitoring have their features and cannot be standardized. Therefore, in each particular case, monitoring is carried out for specific requirements and conditions. The paper presents the results of geospatial monitoring for a part of the UNESCO object Kyiv-Pechersk Lavra. The primary subject of geospatial monitoring is a retaining wall known as the Debosquette Wall. The wall was built in the XVIII century and underwent restoration in 2014. A geospatial monitoring system has been established to prevent undesirable damage and displacements. Assigning the necessary observation accuracy for such a complex object is difficult. In the paper, the modern approach to observation accuracy calculation has been suggested and studied. The approach is based on the application of structural mechanics principles. The structural analysis of the Debosquette Wall has been accomplished. The output of the analysis was applied to calculate the required observation accuracy. The geospatial network and monitoring scheme were developed based on the calculated accuracy. The monitoring proceeded for half a year in 2012-2013, was interrupted for one year, and kept on in 2015. The primary stress was made on the horizontal displacements in that these displacements are the primary threats to the wall stability. The in-depth analysis of the monitoring results has been accomplished. It was found that the displacements have stayed within the allowable values. The developed monitoring approach is recommended for similar projects.

KEYWORDS

Retaining wall, Geospatial monitoring, Observation accuracy, Horizontal displacement, Displacement direction

INTRODUCTION

Geospatial monitoring has become an essential part of most engineering projects. The role and goal of geospatial monitoring depend on the studied structure. Particular attention should be paid to monitoring tasks for historic buildings, especially at the restoration stage. Numerous studies have investigated various monitoring methods depending on the displacements to be measured (vertical, horizontal, or spatial). These methods include different types of leveling, traverses, GNSS, laser scanning, photogrammetry, InSAR, sensors, and their combinations [1-13]. The application of these methods has its pros and cons. However, a number of recent studies have shown that any of these methods can be successfully applied to monitor historic buildings [14-25]. In general, geospatial monitoring of engineering structures contains well-known stages, namely design, target setup, geodetic network creation, observations, data processing, and analysis. This list of stages is well-described in a bunch of papers, reports, and textbooks, e.g., [26,27]. In the case of historic building monitoring, the first stage requires special attention. The design stage supposes the development of recommendations for observation accuracy, network geometry, and observation scheme. Historic buildings stand out in their complex geometry, different and even unknown construction materials, and adverse construction conditions (poorly understood geology, unaccounted loads, etc.). Such conditions lead to an issue of correct accuracy assignment for observations. The traditional approach for accuracy assignment was worked out for typical structures with preliminary known geometry, construction scheme, materials, and loads. Obviously, this case is not applicable to historic buildings. The conditions get complicated in the case of monitoring such complex structures as retaining walls. Retaining walls are used to protect the surrounding structures from possible hill collapse and serve to support the structures placed on the hill. Mostly, retaining walls are considered a kind of anti-landslide structure. Typically, the same methods and approaches are applied for monitoring retaining walls as in a general case. Different studies of monitoring methods for retaining walls have been considered in [28-36]. In our case, the main challenge is monitoring the historic retaining wall. The main theoretical issue that has to be solved is the correct observation accuracy assignment. This task has not been addressed yet in the considered publications. The correct accuracy also serves for the analysis of monitoring results, being that by comparing the allowable accuracy with measured displacements, we may infer the significance of the displacements. Therefore, the paper aimed at the theoretical study of accuracy assignment for monitoring historical retaining walls and practical implementation of the obtained accuracy for monitoring results analysis. The rest of the paper contains a description of the study object, theoretical background for the suggested accuracy assignment approach, a description of monitoring workflow, results of accuracy calculation by the suggested approach, and, finally, the analysis of monitoring results.

MATERIAL AND METHODS

Monitoring object

Kyiv-Pechersk Lavra is one of the astonishing structures of Kyiv city and a world-renowned center of Orthodox Christianity. The Lavra is a complex of various historical structures, including churches, towers, caves, overpasses, and retaining walls. In total, more than fifty structures (Figure 1).

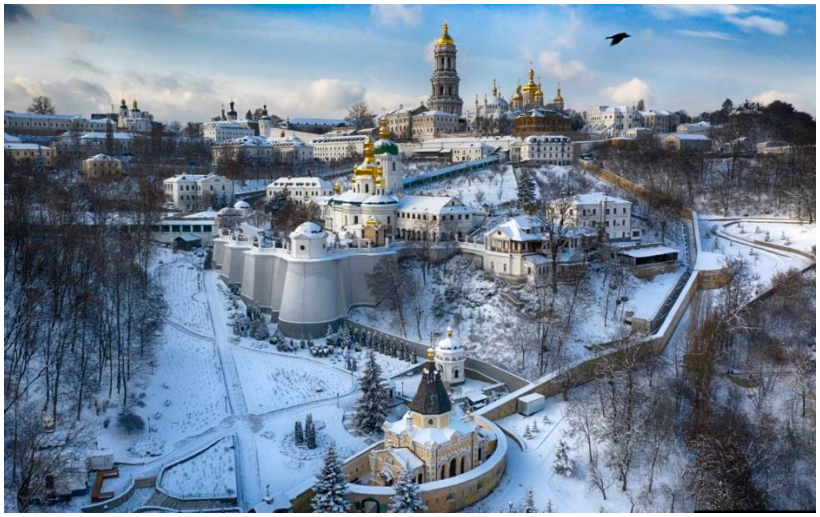

Fig. 1 – General view of the Kyiv-Pechersk Lavra with the Debosquette Wall in front [37]

The history of the Lavra commenced in 1051 when the first complex of cave monasteries was built. The complex developed over many centuries until XIX C. In 1990, the Lavra complex was listed by UNESCO. The main buildings of the Lavra ensemble are the Dormition Cathedral, the Trinity Gate Church, the Great Bell Tower, the Church of All Saints, the Refectory Church, the monastery fortified walls with towers, the cave complexes of St. Anthony (Near) and St. Theodosy (Far) with surface churches, the Exaltation of the Cross and the Nativity of the Virgin and the Church of the Saviour on Berestove [38]. Among the fortified walls, the Debosquette Wall is of great interest [39] (Figure 2).

Fig. 2 – General view of the Debosquette Wall [39]

The wall was built in XVIII C. The total length of the wall exceeds 100 m (Figure 3). Initially, the wall was intended to reinforce the southeast hill of the Near Caves territories. In 1816, two made of bricks rotundas were built at the top of the Debosquette Wall [40].

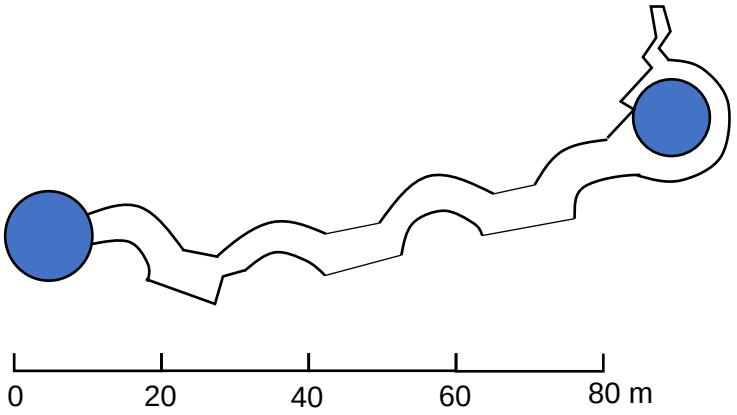

Fig. 3 – Horizontal sketch of the Debosquette Wall

Since its construction as a fortified structure, the primary purpose of the wall has changed. Today, the primary role of the Debosquette Wall is the anti-landslide structure. Therefore, by its functionality, the Debosquette Wall can be treated as a retaining wall that bears the load from a hill, structures emplaced on the hill and prevents them from collapsing. In 2011, the Ukrainian government decided to reconstruct and restore the Debosquette Wall. According to the reconstruction project, complex geospatial monitoring of the wall was envisaged. The goal of the monitoring was to establish the possible displacements of the wall during and right after the restoration works with appropriate accuracy.

Method for monitoring accuracy assignment

Insofar as the monitoring must be accomplished with necessary accuracy, the correct assignment of the accuracy is of great importance. On the other hand, any historical structure is unique, and there is no general approach to monitoring accuracy determination. This is why, before geospatial monitoring works, the appropriate method for accuracy determination has to be developed. It is worth mentioning that the primary attention has to be paid to horizontal displacements for retaining walls. Vertical displacements are typically insignificant. Thus, the method considered below is intended for the accuracy of horizontal displacement determination.

Let us consider the suggested approach for accuracy determination. The right way is the application of structural mechanics principles and approaches. The method presented below further develops the concept suggested in [41,42]. We may consider the wall a vertical cantilever beam clamped at one side and free on another. Under this premise, the deflection will have a maximum value at the top of the wall. Different loads affect the retaining wall. One may find a detailed description of the loads and their relationships in [43]. For our case, we may use the simple model where the main forces are given in Figure 4.

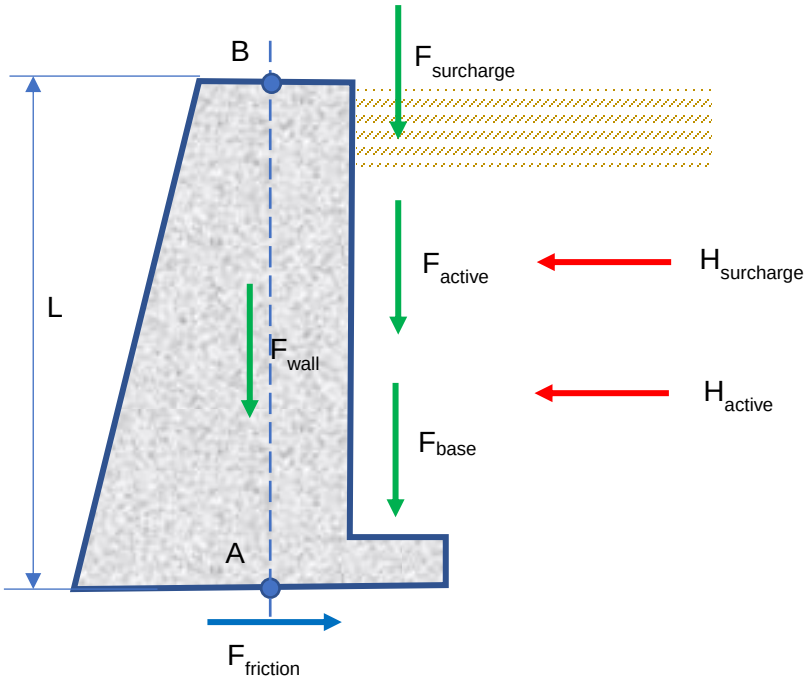

Fig. 4 – Forces acting on a retaining wall

A cantilever retaining wall in Figure 4 must resist both overturning and sliding. In structural mechanics, the normative loads are multiplied by the reliability coefficient. On average, the value of the reliability coefficient can be accepted equals 1.2. In other words, it means that standard loads can exceed the normative loads by 20%. The loads' effect can be presented throughout the overturning moment M_O, which tends to overturn the wall, and sliding force F_S, which tends to move the wall. In terms of the moment, force, and reliability coefficient, we may write down the conditions for allowable deviations in the overturning moment and sliding force. In general, the inequalities

$$M_O \leq M_R, F_S \leq F_R, \tag{1}$$

establish the stability conditions, where M_R, F_R are resisting moment and resisting force. On the other hand, by applying the reliability coefficient, we get

$$\Delta M_O^{max} \leq 0.2 M_O, \Delta F_S^{max} \leq 0.2 F_S \tag{2}$$

Therefore, the values ΔM_O^{max} and ΔF_S^{max} can be treated as additional unpredictable loads that lead to the structure displacement. If we convert the additional loads to displacements δ, we may calculate the necessary accuracy m by using the expression

$$m \leq 0.2\delta. \tag{3}$$

The value m in (3) ensures the observation accuracy for which we can reliably determine the displacements invoked by the additional loads. Thus, the determined displacements will not be distorted by observation accuracy. To calculate the displacement δ, the expressions for the cantilever beam can be used with sufficient accuracy. For the case of distributed force q, given

Young's modulus E and the moment of inertia of the wall's cross-section I, we have [43,44] for the maximum displacement:

$$\delta = \frac{qL^4}{8EI}, \tag{4}$$

for the displacement at any point:

$$\delta(l) = \frac{ql^2(6L^2-4Ll+l^2)}{24EI}, \tag{5}$$

for a slope at any point:

$$\theta(l) = -\frac{ql(3L^2-3Ll+l^2)}{6EI}. \tag{6}$$

For the case of moment, we have a maximum displacement:

$$\delta = \frac{Ma(2L-a)}{2EI}, \tag{7}$$

for the displacement at any point:

$$\delta(l) = \begin{cases} -\frac{Ml^2}{2EI}, l \le a \\ -\frac{Ma^2}{EI}\left(l-\frac{a}{2}\right), l > a, \end{cases} \tag{8}$$

for a slope at any point:

$$\theta(l) = \begin{cases} \frac{Ml}{EI}, l \le a, \\ \frac{Ma^2}{EI}, l > a, \end{cases} \tag{9}$$

where a is a lever arm distance for the moment.

The figures obtained by the expressions (2), (3), (4), (6), (7), and (9) will be provided in the next section.

Accuracy calculation

In the previous section, the method for monitoring accuracy assignment has been suggested. The method allows assigning the accuracy for horizontal displacement determination. Using the necessary initial parameters, one is able to calculate the overturning moment and sliding force for the particular wall. Based on these values, we may calculate the allowable displacement. Let us find out how the suggested method works for the Debosquette Wall. The main initial parameters for calculation are outlined in Table 1. The backfill soil type is stiff clay.

Tab. 1 - Initial data for analysis

Parameter	Value	Parameter	Value
Moment of inertia	1125 m^4	Soil unit weight	13 kN/m^3
Young's modulus	50 MPa	Soil friction angle	30 deg
Wall height	15 m	Wall material strength	20 MPa

Using these data, the overturning moment and sliding force and their allowable deviations were calculated:

$$M_O = 3130\ kN \cdot m,\ F_S = 655\frac{kN}{m},$$

$$\Delta M_O^{max} = 626\ kN \cdot m, \Delta F_S^{max} = 131\frac{kN}{m}.$$

Now, it is possible to use the expressions (4), (6), (7), and (9) to calculate the displacements due to the overturning moment and sliding force. The displacement and slope graphs for the overturning moment and sliding force are presented in Figure 5 and Figure 6, as well as the moment diagrams for both cases.

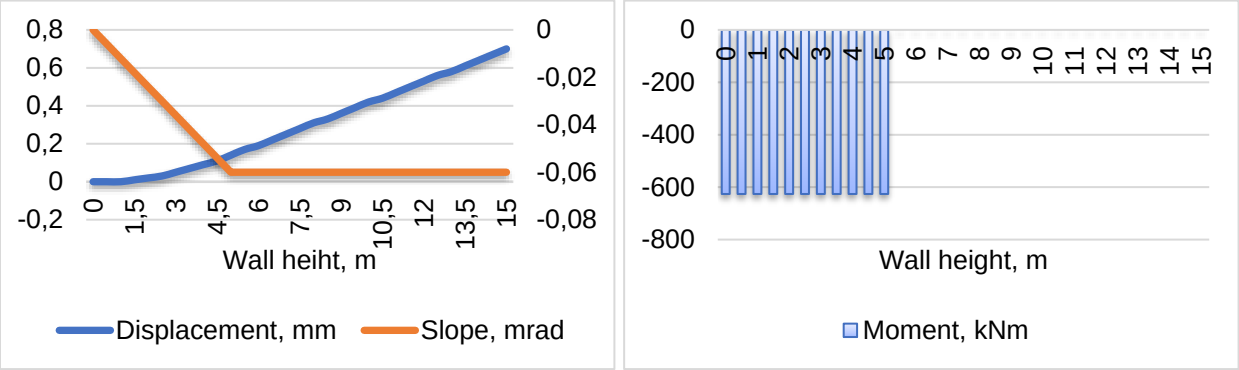

Fig. 5 – Overturning moment effect

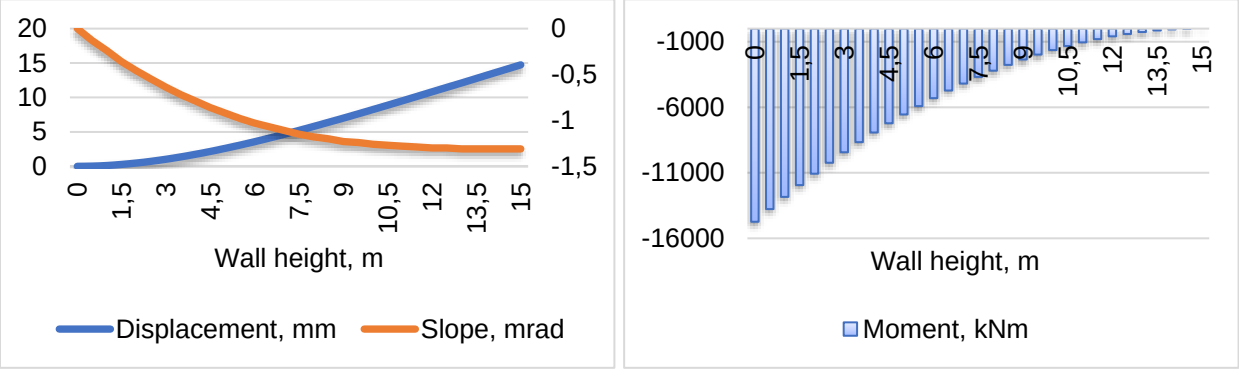

Fig. 6 – Sliding force effect

We may apply the superposition method to calculate the final displacement, which gives a preliminary result for a displacement of 15.44 mm. For monitoring accuracy calculation, this approximation provides reasonable output. Therefore, the observation accuracy will

$$m = 0.2 \cdot 15.44 = 3.1\ mm.$$

This value was used as reference accuracy for developing the observation scheme and measurement equipment choice. The chosen equipment for measurements is capable of ensuring the determined accuracy. The estimated value of the total displacement δ was applied for measurement result analysis.

Monitoring scheme

Geospatial monitoring has been accomplished separately for vertical and horizontal displacements. To these aims, two different monitoring networks were created. For the horizontal monitoring network, the Kyiv city coordinate system was adopted. GNSS observations referenced the point of beginning for the horizontal network to the city coordinate system. In what follows, the initial coordinates were accepted unchanged. All points of the horizontal monitoring network were permanently mounted by tube pillars with screw holes for precise centering of total stations and targets. The scheme of the horizontal network is given in Figure 7. The distances and angles were measured by Leica TCR 1201+ R400 total station, which has an angle measurement error ±1 sec, and distance measurement error ±1 mm + 1.5 ppm. The distances and angles were measured with six repetitions. The network was checked with control measurements for each observation epoch to control network point displacements. Deformation targets were mounted onto the wall along three levels (see Figures 8 and 9). The bottom-level targets (Rp1 – Rp23) were used both for vertical and horizontal displacement determination. In total, sixty-three targets were mounted.

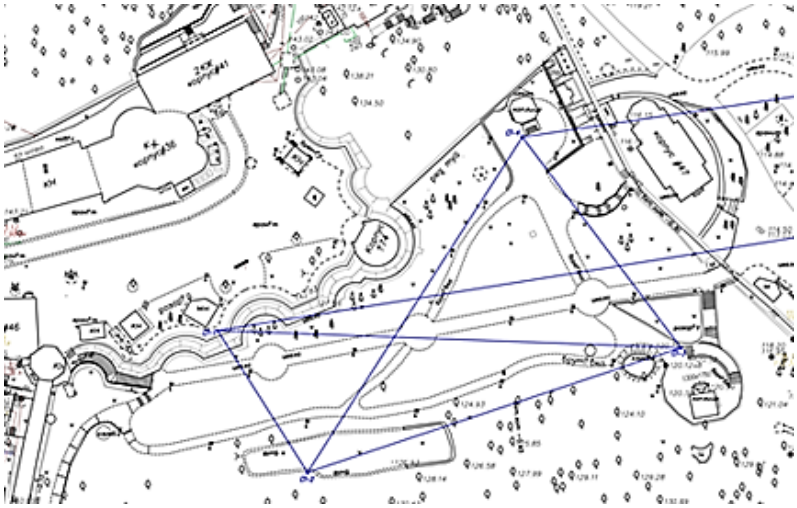

Fig. 7 – Scheme of the horizontal monitoring network

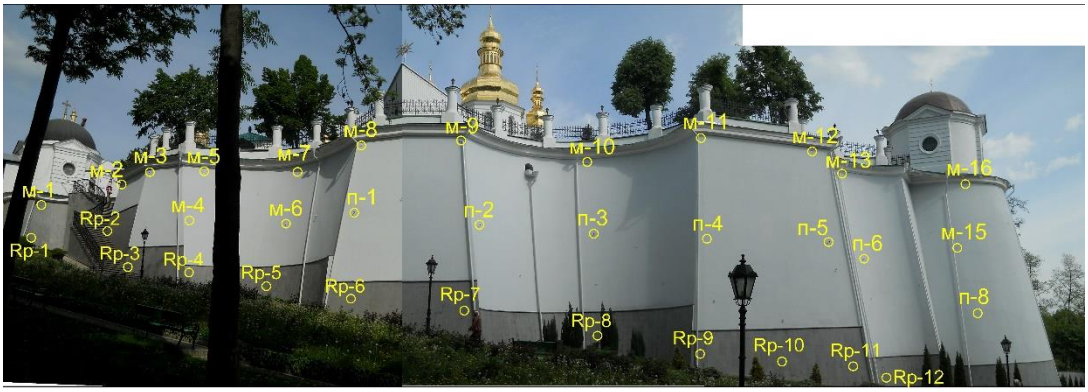

Fig. 8 – Scheme of the deformation targets (southern facade)

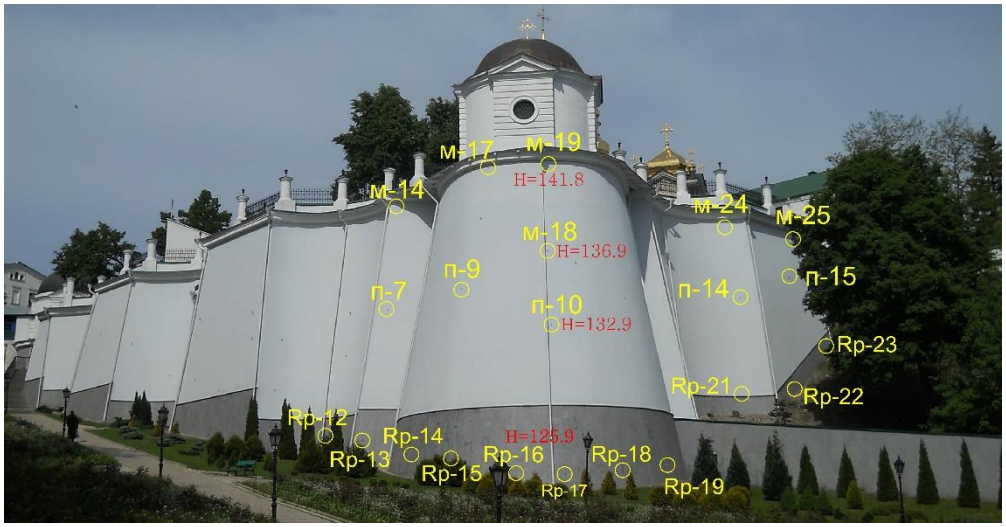

Fig. 9 – Scheme of the deformation targets (southeastern facade)

The vertical monitoring network was referenced to the benchmarks of the city height system using standard leveling procedures. The scheme of the vertical monitoring network is given in Figure 10.

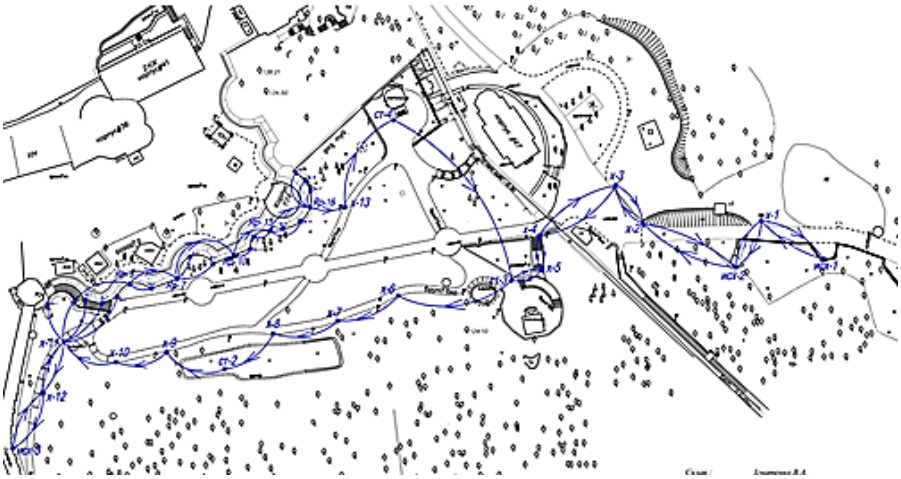

Fig. 10 – Scheme of the vertical monitoring network

Points of beginning for the vertical network were placed outside the region of possible deformations. Levelling lines were run in forward and inverse directions. The precise level DL-101C (levelling error for one kilometer of a double run is ± 0.4 mm) and coded invar level rods were used. Lines of sight were in a range of 25 m.

The results of monitoring will be presented in the next section. But one remark has to be provided. It was determined that vertical displacements were insignificant during the monitoring period. The maximum value was detected for target Rp 23 and equals -3 mm. That is why only horizontal displacements will be considered and analyzed in what follows.

RESULTS

Monitoring results

The monitoring was carried out according to the schemes considered in the previous section. The observation accuracy corresponded to the value calculated before. The dataset for monitoring the Debosquette Wall spans the period from 05.11.2012 until 13.05.2015p. During that time interval, twenty observations were accomplished. As it was mentioned, the main concern was horizontal displacements. Below, the horizontal displacements for different deformation targets are presented.

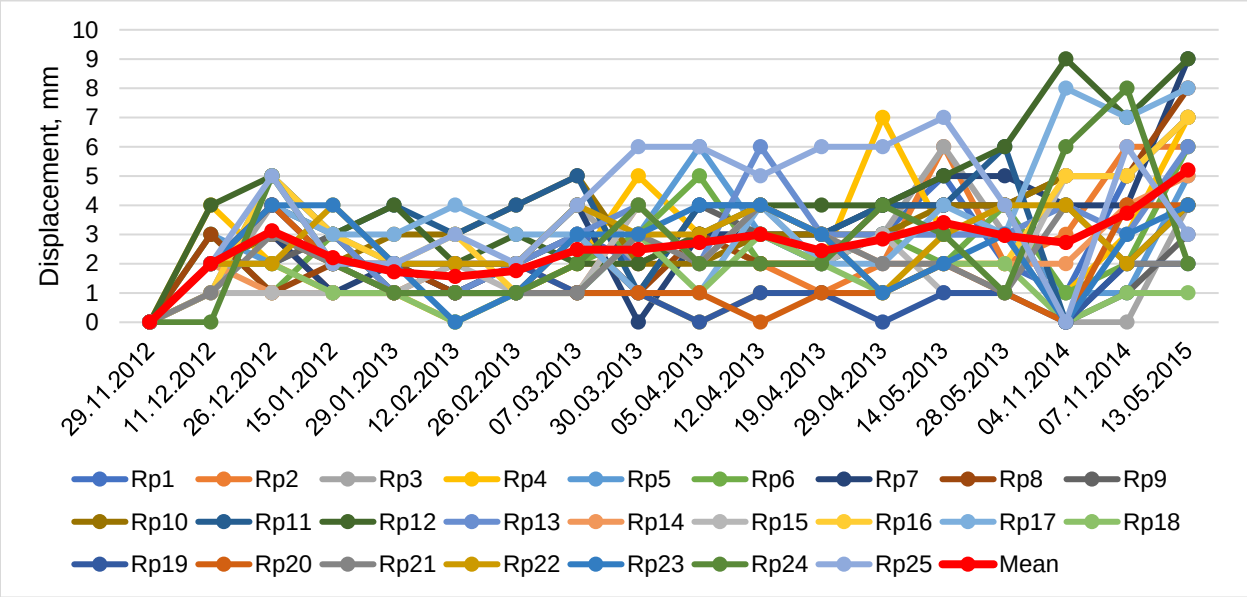

Fig. 11 – Horizontal displacements for deformation targets Rp1 – Rp25

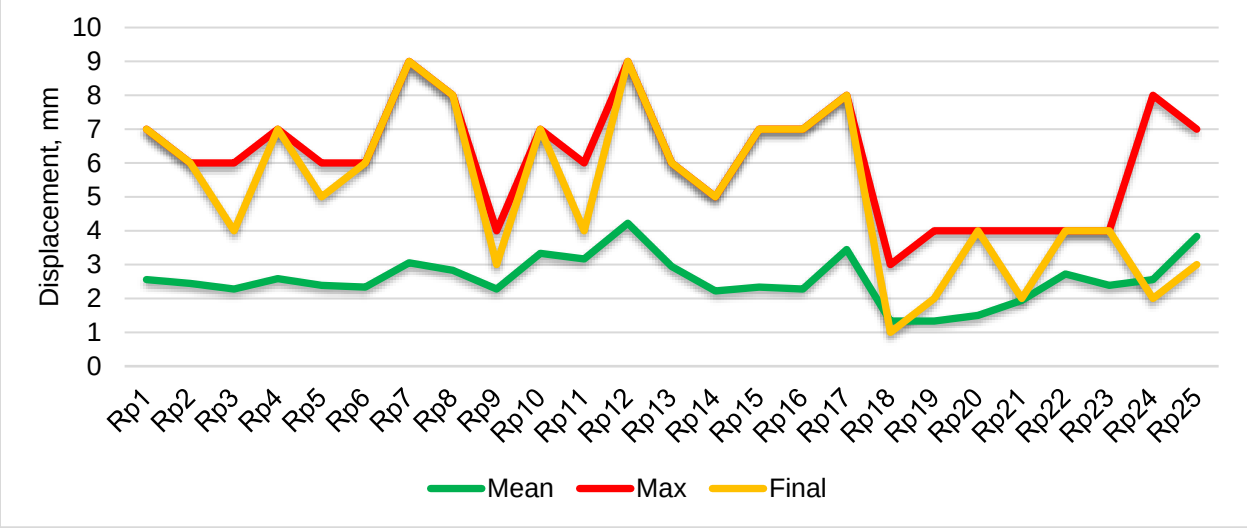

Fig. 12 – Main characteristics of the deformation process for targets Rp1 – Rp25

In Figure 11, the mean displacement for each observation epoch is given aside from the horizontal displacements. Figure 12 shows each deformation target's mean, maximum, and final displacement. The same content is given in Figure 13 – Figure 16 but for different deformation targets.

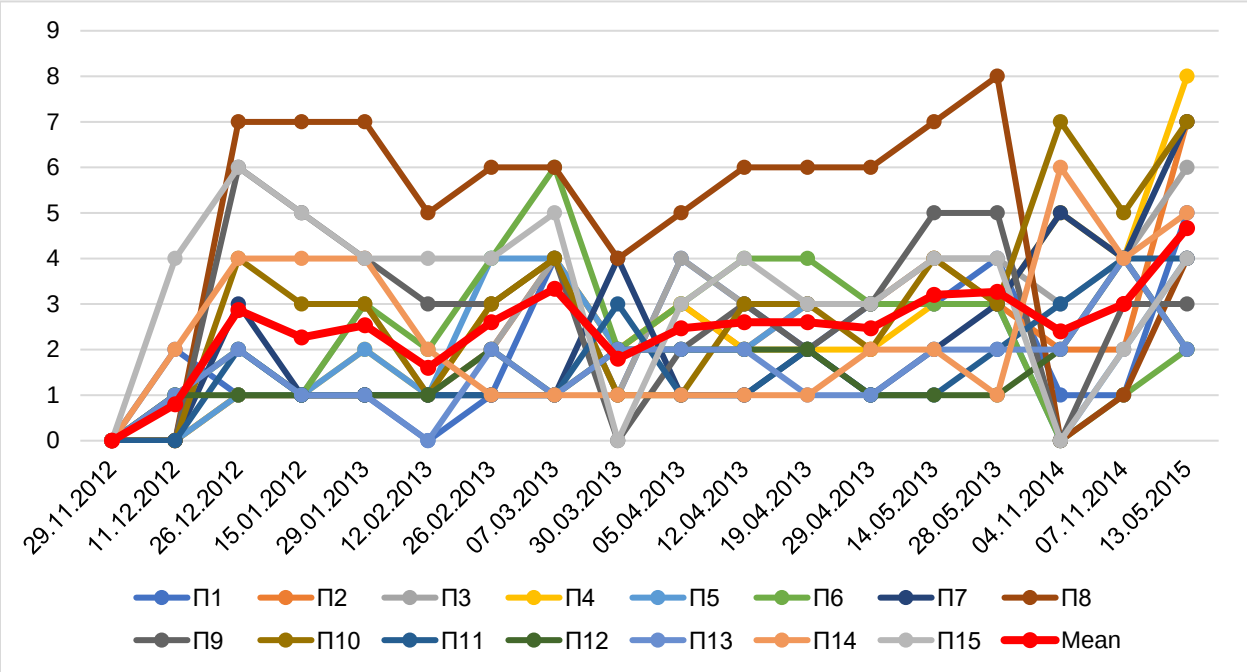

Fig. 13 – Horizontal displacements for deformation targets П1 – П15

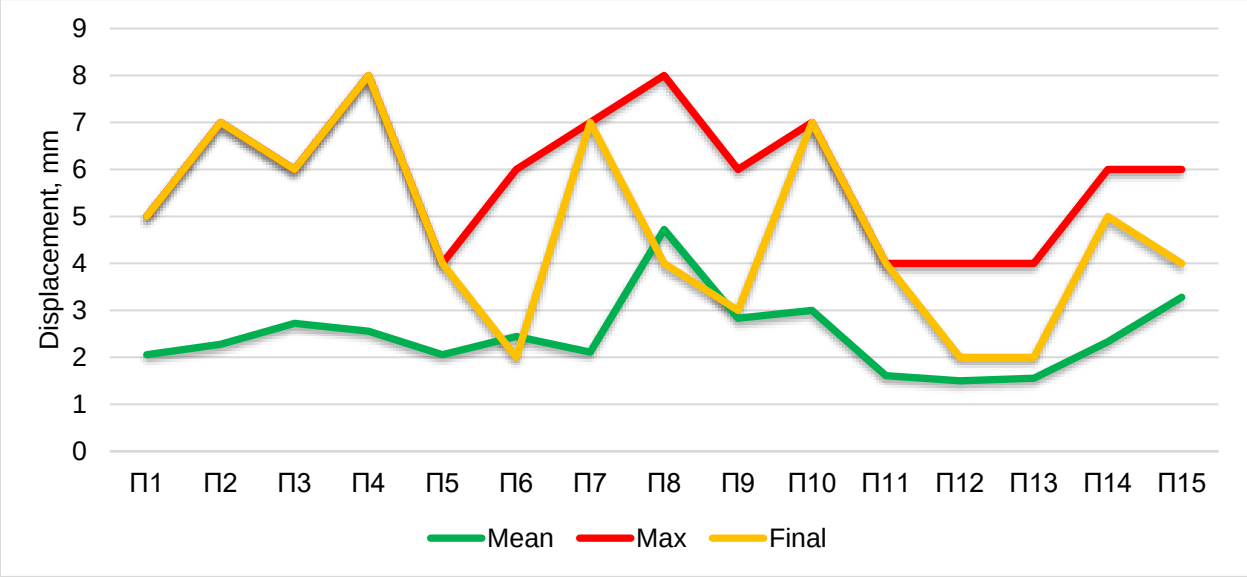

Fig. 14 – Main characteristics of the deformation process for targets П1 – П15

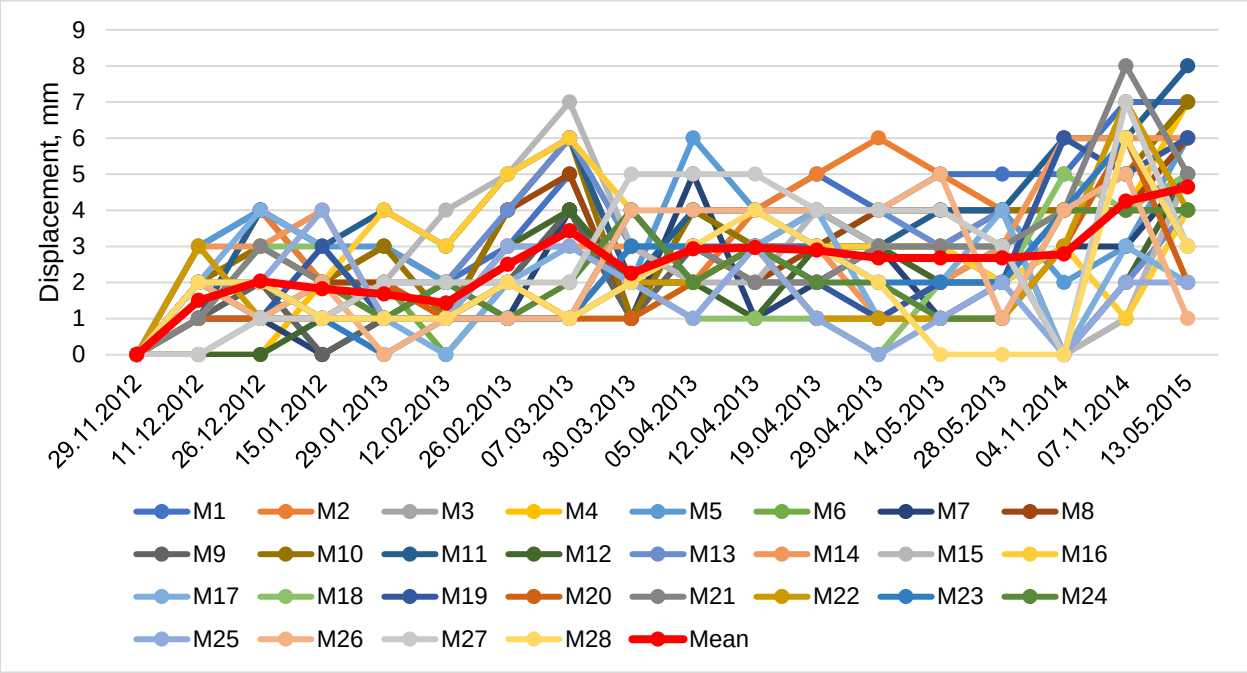

Fig. 15 – Horizontal displacements for deformation targets M1 – M28

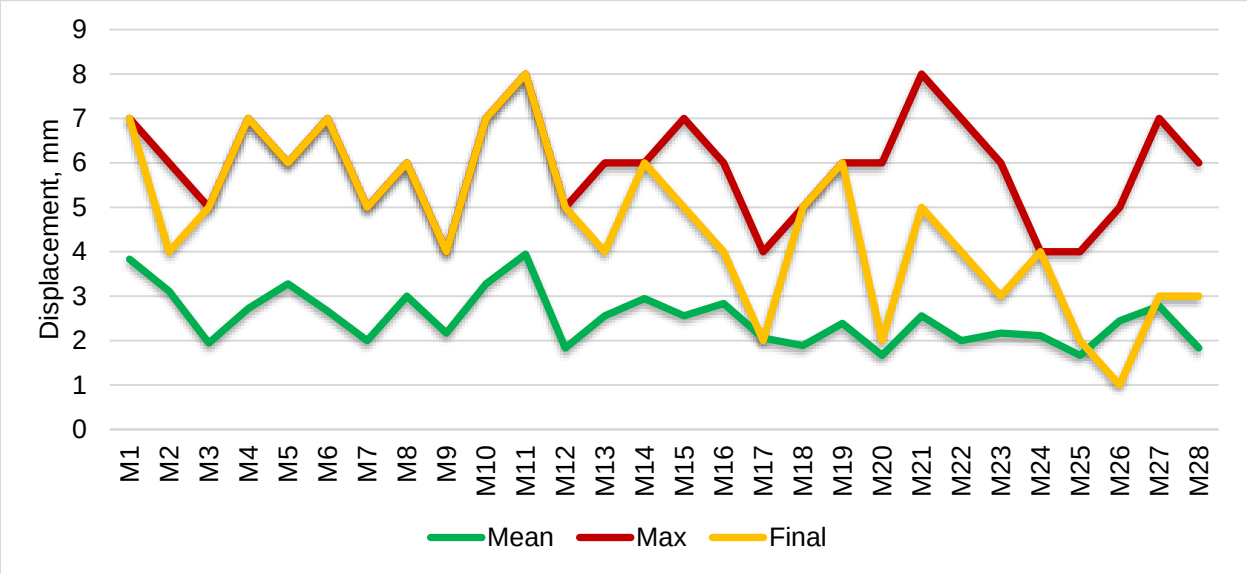

Fig. 16 – Main characteristics of the deformation process for targets M1 – M28

The results presented in Figure 11 – Figure 16 yielded some interesting findings. Firstly, the largest displacements have reached the targets in the bottom of the Debosquette Wall, namely 7 mm for the targets Rp1, Rp4, Rp10, Rp15, Rp16; 8 mm for the targets Rp8, Rp17, and 9 mm for the targets Rp7, Rp12. Just a few targets in the middle and at the top of the retaining wall had significant horizontal displacements, specifically 7 mm for the targets П2, П7, M1, M6, M10, M18, and 8 mm for the targets П4, M11. Secondly, none of the displacements reached the critical value

of 15 mm. Thirdly, the last observation epochs have shown that the displacements tend to increase after the reconstruction. That is especially clear in Figure 11 and Figure 13. The latter inference makes indispensable further monitoring both for vertical and horizontal displacements.

CONCLUSION

Current research appears to validate the view that the geospatial monitoring of historic structures is a unique process. Performing geospatial monitoring needs a neat approach and correct estimation of the task and solutions. The paper considered the particular case of the geospatial monitoring of historic retaining walls before and after their reconstruction. The crucial point of such monitoring is a correct observation accuracy assignment. It was suggested to assign the proper accuracy using principles of structural mechanics. The aim of this approach is twofold: to determine the necessary observation accuracy and to obtain the correct criterion for monitoring data analysis. The appropriate monitoring workflow was suggested and implemented based on the calculated accuracy. Thanks to the correct choice of monitoring accuracy, the high reliability of the measurements was ensured. The results of monitoring have confirmed the relative stability of the studied historic structure. However, the displacements tend to increase, which requires monitoring to keep on. Future studies will have to further the fusion of structural mechanics and applied geodesy for monitoring tasks.

REFERENCES

[1] Acosta L.E., De Lacy, M.C., Ramos, M.I., Cano, J.P., Herrera, A.M., Avilés, M., Gil, A.J. 2018. Displacements study of an earth fill dam based on high precision geodetic monitoring and numerical modeling. Sensors, 18(5): 1369-1384. https://doi.org/10.3390/s18051369

[2] Aminjafari S. 2017. Monitoring of Masjed-Soleiman embankment dam's deformation using a combination of interferometric synthetic aperture radar (InSAR) and finite element modeling. Journal of Geodesy and Cartography, 43(1): 14-21. https://doi.org/10.3846/20296991.2017.1299842

[3] Janowski A., Kaminski W., Makowska K., Szulwic J., Wilde K. 2015. The method of measuring the membrane cover geometry using laser scanning and synchronous photogrammetry. In: Proccedings of the 15th International Multidisciplinary Scientific GeoConference - SGEM2015. 1-11.

[4] Shen N., Chen L., Liu J., Wang L., Tao T., Wu D., Chen R. 2019. A review of global navigation satellite system (GNSS)-based dynamic monitoring technologies for structural health monitoring. Remote Sensing, 11: 1001-1046. https://doi.org/10.3390/rs11091001

[5] Taşçi L. 2015. Deformation monitoring in steel arch bridges through close-range photogrammetry and the finite element method. Experimental Techniques, 39: 3-10. https://doi.org/10.1111/ext.12022

[6] Jiménez-Martínez M.J., Quesada-Olmo N., Zancajo-Jimeno J.J., Mostaza-Pérez T. 2023. Bridge Deformation Analysis Using Time-Differenced Carrier-Phase Technique. Remote Sensing, 15: 1458. https://doi.org/10.3390/rs15051458

[7] Caldera, S., Barindelli S., Sansò F., Pardi L. 2022. Monitoring of Structures and Infrastructures by Low-Cost GNSS Receivers. Applied Sciences, 12: 12468. https://doi.org/10.3390/app122312468

[8] Sztubecki J., Topoliński S., Mrówczyńska M., Bağrıaçık B., Beycioğlu A. 2022. Experimental Research of the Structure Condition Using Geodetic Methods and Crackmeter. Applied Sciences, 12: 6754. https://doi.org/10.3390/app12136754

[9] Xiao P., Zhao R., Li D., Zeng Z., Qi S., Yang X. 2022. As-Built Inventory and Deformation Analysis of a High Rockfill Dam under Construction with Terrestrial Laser Scanning. Sensors, 22: 521. https://doi.org/10.3390/s22020521

[10] Kovačič B., Doler D., Topolšek D. 2021. Optimization and Development of the Model for Monitoring the Deformations on the Airport Runways. Processes, 9: 833. https://doi.org/10.3390/pr9050833

[11] Stiros S.C. 2021. GNSS (GPS) Monitoring of Dynamic Deflections of Bridges: Structural Constraints and Metrological Limitations. Infrastructures, 6: 23. https://doi.org/10.3390/infrastructures6020023
[12] Scaioni M., Marsella M., Crosetto M., Tornatore V., Wang J. 2018. Geodetic and Remote-Sensing Sensors for Dam Deformation Monitoring. Sensors, 18: 3682. https://doi.org/10.3390/s18113682
[13] Erol B. 2010. Evaluation of High-Precision Sensors in Structural Monitoring. Sensors, 10: 10803-10827. https://doi.org/10.3390/s101210803
[14] Barazzetti L., Banfi F., Brumana R., Gusmeroli G., Previtali M., Schiantarelli G. 2015. Cloud-to-BIM-to-FEM: Structural simulation with accurate historic BIM from laser scans. Simulation Modelling Practice and Theory, 57: 71-87. http://dx.doi.org/10.1016/j.simpat.2015.06.004
[15] Castagnetti C., Cosentini R.M., Lancellotta R., Capra A. 2017. Geodetic monitoring and geotechnical analyses of subsidence induced settlements of historic structures. Struct Control Health Monitoring, 24: 1-15. https://doi.org/10.1002/stc.2030
[16] Rossi M., Bournas D. 2023. Structural Health Monitoring and Management of Cultural Heritage Structures: A State-of-the-Art Review. Applied Sciences, 2023: 13, 6450. https://doi.org/10.3390/app13116450
[17] Casula G., Fais S., Cuccuru F., Bianchi M.G., Ligas P. 2023. Diagnostic Process of an Ancient Colonnade Using 3D High-Resolution Models with Non-Invasive Multi Techniques. Sensors, 23: 3098. https://doi.org/10.3390/s23063098
[18] Bačová D., Ižvoltová J., Šedivý Š., Chromčák J. 2023. Different Approach for the Structure Inclination Determination. Buildings, 13: 637. https://doi.org/10.3390/buildings13030637
[19] Costanzo A., Falcone S., La Piana C., Lapenta V., Musacchio M., Sgamellotti A., Buongiorno M.F. 2022. Laser Scanning Investigation and Geophysical Monitoring to Characterise Cultural Heritage Current State and Threat by Traffic-Induce Vibrations: The Villa Farnesina in Rome. Remote Sensing, 14: 5818. https://doi.org/10.3390/rs14225818
[20] Patrucco G., Gómez A., Adineh A., Rahrig M., Lerma J.L. 2022. 3D Data Fusion for Historical Analyses of Heritage Buildings Using Thermal Images: The Palacio de Colomina as a Case Study. Remote Sensing, 14: 5699. https://doi.org/10.3390/rs14225699
[21] Miano A., Di Carlo F., Mele A., Giannetti I., Nappo N., Rompato M., Striano P., Bonano M., Bozzano F., Lanari R., et al. 2022. GIS Integration of DInSAR Measurements, Geological Investigation and Historical Surveys for the Structural Monitoring of Buildings and Infrastructures: An Application to the *Valco San Paolo* Urban Area of Rome. Infrastructures, 7: 89. https://doi.org/10.3390/infrastructures7070089
[22] Giuffrida D., Bonanno S., Parrotta F., Mollica Nardo V., Anastasio G., Saladino M.L., Armetta F., Ponterio R.C. 2022. The Church of S. Maria Delle Palate in Tusa (Messina, Italy): Digitization and Diagnostics for a New Model of Enjoyment. Remote Sensing, 14: 1490. https://doi.org/10.3390/rs14061490
[23] Del Soldato M., Farolfi G., Rosi A., Raspini F., Casagli N. 2018. Subsidence Evolution of the Firenze–Prato–Pistoia Plain (Central Italy) Combining PSI and GNSS Data. Remote Sensing, 10: 1146. https://doi.org/10.3390/rs10071146
[24] Sánchez-Aparicio L.J., Villarino A., García-Gago J., González-Aguilera D. 2016. Photogrammetric, Geometrical, and Numerical Strategies to Evaluate Initial and Current Conditions in Historical Constructions: A Test Case in the Church of San Lorenzo (Zamora, Spain). Remote Sensing, 8: 60. https://doi.org/10.3390/rs8010060
[25] Fregonese L., Barbieri G., Biolzi L., Bocciarelli M., Frigeri A., Taffurelli L. 2013. Surveying and Monitoring for Vulnerability Assessment of an Ancient Building. Sensors, 13: 9747-9773. https://doi.org/10.3390/s130809747
[26] Eichhorn A. 2007. Tasks and newest trends in geodetic deformation analysis: a tutorial. In Proceedings of the 15th European Signal Processing Conference (EUSIPCO 2007), Poznan, Poland, 1156-1160.
[27] Welsch W.M., Heunecke O. 2001. Models and terminology for the analysis of geodetic monitoring observations - Official Report of the Ad-Hoc Committee of FIG Working Group 6.1. In Proceedings of the 10th FIG International Symposium on Deformation Measurements, Orange, California, USA. 390-412.

[28] Oats R.C., Escobar-Wolf R., Oommen T. 2017. A Novel Application of Photogrammetry for Retaining Wall Assessment. Infrastructures, 2: 10. https://doi.org/10.3390/infrastructures2030010
[29] Sestras P., Bilașco Ș., Roșca S., Veres I., Ilies N., Hysa A., Spalević V., Cîmpeanu S.M. 2022. Multi-Instrumental Approach to Slope Failure Monitoring in a Landslide Susceptible Newly Built-Up Area: Topo-Geodetic Survey, UAV 3D Modelling and Ground-Penetrating Radar. Remote Sensing, 14: 5822. https://doi.org/10.3390/rs14225822
[30] Peduto D., Oricchio L., Nicodemo G. et al. 2021. Investigating the kinematics of the unstable slope of Barberà de la Conca (Catalonia, Spain) and the effects on the exposed facilities by GBSAR and multi-source conventional monitoring. Landslides, 18: 457–469. https://doi.org/10.1007/s10346-020-01500-9
[31] Kaartinen E., Dunphy K., Sadhu A. 2022. LiDAR-Based Structural Health Monitoring: Applications in Civil Infrastructure Systems. Sensors, 22: 4610. https://doi.org/10.3390/s22124610
[32] Scotland I., Dixon N., Frost M.W., Wackrow R., Fowmes G.J., Horgan G. Measuring Deformation Performance of Geogrid Reinforced Structures Using a Terrestrial Laser Scanner; Loughborough University Institutional Repository: Leicestershire, UK, 2014.
[33] Tung S.H., Weng M.C., Shih M.H. 2013. Measuring the in situ deformation of retaining walls by the digital image correlation method. Engineering. Geology, 166: 116–126. https://doi.org/10.1016/j.enggeo.2013.09.008
[34] Scaioni M., Alba M., Roncoroni F., Giussani A. 2010. Monitoring of a SFRC retaining structure during placement. Eur. J. Environ. Civ. Eng., 14: 467–493 https://doi.org/10.1080/19648189.2010.9693237
[35] Laefer D., Lennon D. 2008. Viability Assessment of Terrestrial LiDAR for Retaining Wall Monitoring. GeoCongress, 310: 247-254. https://doi.org/10.1061/40971(310)
[36] Oskouie P., Becerik-Gerber B., Soibelman L. 2016. Automated measurement of highway retaining wall displacements using terrestrial laser scanners. Autom. Constr., 65: 86–101. https://doi.org/10.1016/j.autcon.2015.12.023
[37] Inside Kyiv's Sacred Cave Monastery As 'Eviction' Deadline Looms. Available online: https://www.rferl.org/a/kyiv-monastery-lavra-eviction-crisis/32319718.html (accessed on 01 August 2023)
[38] Report of Joint World Heritage Centre/ICOMOS Reactive Monitoring Mission to the World Heritage property. Kyiv: Saint-Sophia Cathedral and Related Monastic Buildings, Kyiv-Pechersk Lavra (Ukraine). Available online: http://kyiv-heritage.com/sites/default/files/Ukraine-Kyiv-RM%20mission%20WHC-ICOMOS-14FEB20%20332c%20(ALL).pdf (accessed on 01 August 2023)
[39] Kyiv-Pechersk Lavra. Part 9. Other objects. Available online: https://ukrainaincognita.com/kyivska-oblast/kyiv/kyevo-pecherska-lavra/kyevo-pecherska-lavra-chastyna-9-inshi-obekty (accessed on 01 August 2023)
[40] Debosquette wall. Available online: https://uk.wikipedia.org/wiki/%D0%9C%D1%83%D1%80_%D0%94%D0%B5%D0%B1%D0%BE%D1%81%D0%BA%D0%B5%D1%82%D0%B0 (accessed on 29 July 2023)
[41] Shults, R., 2021. The Models of Structural Mechanics for Geodetic Accuracy Assignment: A Case Study of the Finite Element Method. In Contributions to International Conferences on Engineering Surveying. Springer Proceedings in Earth and Environmental Sciences. Springer, Cham, edited by A. Kopáčik, P. Kyrinovič, J. Erdélyi, R. Paar, A. Marendić, 187-197. https://doi.org/10.1007/978-3-030-51953-7_16
[42] Shults, R., 2022. Structural analysis of monitoring results of long-span roof structures. In: Proceedings of the 5th Joint International Symposium on Deformation Monitoring (JISDM), Valencia, Spain, 431-438. http://doi.org/10.4995/JISDM2022.2022.13893
[43] Connor, J.J., & Faraji, S. 2016. Fundamentals of structural engineering (2nd ed). Springer. https://doi.org/10.1007/978-3-319-24331-3
[44] Clayton C.R., Woods R.I., Bond A.J., Milititsky J. 2014. Earth Pressure and Earth-Retaining Structures. CRC Press.